Available at www.sciencedirect.com

ScienceDirect

journal homepage: www.elsevier.com/locate/issn/15375110

Research Paper: AE—Automation and Emerging Technologies

Recognition and classification of external skin damage in citrus fruits using multispectral data and morphological features

J. Blasco[a,*], N. Aleixos[b], J. Gómez-Sanchís[c], E. Moltó[a]

[a]Centro de Agroingeniería. Instituto Valenciano de Investigaciones Agrarias (IVIA). Ctra. Moncada-Náquera km 5, 46113 Moncada (Valencia), Spain.

[b]Instituto en Bioingeniería y Tecnología Orientada al Ser Humano. Universidad Politécnica de Valencia. Camino de Vera s/n, 46022 Valencia, Spain

[c]Intelligent Data Analysis Laboratory, IDAL, Electronic Engineering Department, Universidad de Valencia Dr. Moliner 50, 46100 Burjasot, Valencia, Spain

ARTICLE INFO

Article history:
Received 24 July 2008
Received in revised form
19 March 2009
Accepted 23 March 2009
Published online 21 April 2009

The computer vision systems currently used for the automatic inspection of citrus fruits are normally based on supervised methods that are capable of detecting defects on the surface of the fruit but are unable to discriminate between different types of defects. Identifying the type of the defect affecting each fruit is very important in order to optimise the marketing profit and to be able to take measures to prevent such defects from occurring in the future. In this paper, we present a computer vision system that was developed for the recognition and classification of the most common external defects in citrus. In order to discriminate between 11 types of defects, images of the defects were acquired in five spectral areas, including the study of near infrared reflectance and ultraviolet induced fluorescence. The system combines spectral information about the defects with morphological estimations of them in order to classify the fruits in categories. The fruit-sorting algorithm proposed here was tested by using it to identify the defects in more than 2000 citrus fruits, including mandarins and oranges. The overall success rate reached 86%.

1. Introduction

The overall appearance of any object is a combination of its chromatic attributes (colour) and its geometric attributes (such as gloss or shininess, shape, texture, haze and translucency), together with the presence of defects or damage that can devalue the external quality. Thus, both types of attributes should be measured and accounted for when making visual or instrumental assessments of appearance (Batchelor and Whelan, 1995). The purpose of computer vision systems is to aid or enhance tasks normally performed by humans, such as the quality evaluation of fruit. Consumers have developed strong associations through appearance and base their pre-purchase judgments of taste and quality on the appearance of the product. The food industry is also limited by governmental regulations concerning quality. In this

* Corresponding author.
E-mail address: blasco_josiva@gva.es (J. Blasco).
1537-5110/$ – see front matter © 2009 IAgrE. Published by Elsevier Ltd. All rights reserved.
doi:10.1016/j.biosystemseng.2009.03.009

context, appearance measurement techniques must be used to ensure good external quality of produce that meets the quality standards. Blasco *et al.* (2003) developed a computer vision system capable of detecting external features such as size, shape and external defects in peaches, apples and citrus, and separating them according to pre-programmed quality rules. Current commercial systems for fruit inspection based on machine vision are capable of detecting skin defects, but automatic recognition of such defects is still a major challenge. Identification is needed so that the seriousness of the damage can be evaluated, since some blemishes may only imply a slight reduction in the value of the product but others, like those produced by fungal infections, can lead to considerable deterioration of the merchandise during its conservation and marketing. By identifying the type of each defect individually, the economic performance of the fruit can be optimised and measures can be adopted to prevent such flaws in the future.

Computer vision systems have been employed mainly to automate visual inspection in the industry (Ponsa *et al.*, 2003). One particular implementation is the inspection of the quality of biological products, which has specific problems such as the natural variability in the colour, shapes, sizes and environments of these products, as stated by Zheng *et al.* (2006) in an extensive review of these applications. The selection of a particular method to process an image can depend on restrictions imposed by the problem. For example, the segmentation algorithms commonly implemented in commercial automatic systems for fruit grading are restricted by the processing time and so they are mostly based on fast pixel-oriented techniques. In these techniques, the value of each individual pixel is normally used as the only feature for segmenting the image. Simpler techniques are based on thresholding, when the objects of interest are well contrasted against the background and a high processing speed is required. Bennedsen *et al.* (2005) used this method to segment several images of apples acquired while they were rotating and crossing an inspection chamber.

Colour images need a more sophisticated segmentation that allows the different colour coordinates of each pixel to be combined to produce a single result. For example, Blasco *et al.* (2002) used Bayesian discriminant analysis to classify each pixel in to one of the predefined classes in order to detect weeds in the field. Subsequent morphological operations allowed weeds and crops to be differentiated. Aleixos *et al.* (2002) presented a system for the analysis of colour images of citrus in real time using pixel-oriented segmentation. Despite the use of digital signal processors as specific image analysis hardware, the use of a rapid segmentation technique was required to obtain real-time data.

These techniques have to learn how to relate the colour of pixels to regions and, thus, a representative dataset is necessary to train the classifier. A typical training method is described by Al-Mallahi *et al.* (2008), who sampled pixels belonging to different tuber potatoes to build a classifier based on discriminant analysis. These techniques segment the images quickly, but they need long training sessions and are sensitive to changes in the colour of the objects, which can vary significantly between different cultivars or even in fruits of the same cultivar harvested in different groves. Moreover, they only discriminate between defects and sound skin, and give information about the number of defects or the global defective area but not about the type of each defect.

Currently, there are no commercial computer vision systems for citrus fruit inspection that are capable of identifying the type of defect that is affecting the fruit, since they normally use only colour information from the images to achieve real-time operation. As some external defects of citrus have a similar colour, it is difficult to distinguish between different types of defects using only this feature. The regularity of the shape of different defects, and especially the size, varies from one type of defect to another, thus making them features that may be suitable for distinguishing between different defects. The identification of the kind of defect would make it possible to create automatic systems to discriminate between sound fruits, fruits with slight skin defects that can be marketed as second categories and fruits with damage such as decay, which may develop and spread to other fruits. These defects must be detected early and the affected fruit separated from the rest.

Other works have demonstrated the value of non-visible imaging in the inspection of fruit quality (Mehl *et al.*, 2000; Alchanatis *et al.*, 1999; Bennedsen and Peterson, 2005). A system for detecting defects, which includes some severe types of damage such as black rot and decay, was set up by Ariana *et al.* (2006). They found that the combination of visible and near-infrared (NIR) reflectance and ultraviolet-induced fluorescence (UVFL) was more effective in the detection of most defects than the same systems used separately. In a previous work, Blasco *et al.* (2007a) combined UV, visible and NIR reflectance and UVFL to detect external defects in citrus. However, the use of ultraviolet light is not justified by the limited contribution of this system to the final result, in addition to its high complexity and the fact that it can be harmful for the operators. In this regard, Gómez-Sanchis *et al.* (2008a) studied the possibility of avoiding the use of ultraviolet light and using only visible and NIR reflectance to detect damage caused by rot in citrus. They analysed the reflectance of the damage in several visible and NIR wavelengths using a hyperspectral image acquisition system.

Multispectral and morphological information is used in this paper to develop a fruit-sorting algorithm for classifying the fruits according to the type of defects they present. Our work also studies the contribution of non-visible information to the identification of some citrus defects and proposes a computer vision system that uses visible colour and NIR reflectance and UVFL to detect and recognise the defects.

2. Objective

The objective of this work is to identify the type of external defects in citrus using multispectral computer vision. Spectral and morphological parameters such as colour, area, length, width or the fast Fourier transform (FFT) of the radius signature of the perimeter have to be calculated. This information has to be combined to identify and distinguish between different types of defects and to sort the fruit taking into account the severity of the defects.

3. Material and methods

3.1. Fruit and defect samples

This work is aimed at identifying the type of different defects of citrus fruits once they have been detected and separated from the sound skin using image segmentation methods like the one described in Blasco *et al.*, (2007b). For this reason, a total of 2132 oranges and mandarins each containing skin defects were collected at random from a packing line and imaged using the acquisition systems described below, thus giving a total of 10660 images of defects. This set was used to obtain the results presented in this work. A different set consisting of 10 images for each type of defect acquired with each spectral system ($10 \times 5 \times 11 = 550$ images) was acquired and used to train the algorithms. The defects found on the fruits were described as those that only affect the appearance of the fruit, such as oleocellosis, chilling injury, sooty mould, phytotoxicity, scales, scarring, thrips, and other defects with greater economic importance, such as anthracnose, stem-end injury, green mould (decay caused by *Penicillium digitatum*) and medfly (*Ceratitis capitata*) (Wiedemann) egg deposition. Their sizes vary from large defects, such as anthracnose or chilling injury, to small ones like scales or medfly. The colour also differs from one to another and may range from the white of stem-end injury, the silver or grey of thrips, the orange or green of *P. digitatum* or the brown of oleocellosis to the black of anthracnose. A detailed view of representative defects in each class is shown in Fig. 1.

Figure 2 shows the frequency distribution of the defects. The differences in the representation of each type of defect can be explained by the high rate at which some defects appear on commercial packing lines, as is the case of scarring or thrips scarring, and the appearance of other defects that are composed of multiple stains or lesions in the skin of the same fruit, each of which is taken as a single defect (phytotoxicity, scales).

3.2. Acquisition of the images

Images of the same fruit were acquired using three different systems: visible and NIR reflectance, and fluorescence. Two VIS and NIR sensitive cameras were used to acquire all the images. A progressive scan colour camera was used to acquire fluorescence and visible images, which consisted of three monochromatic images of red, green and blue (RGB) wavelengths. The equipment used to acquire all the images is described in detail in Blasco *et al.* (2007a). Basically, the colour image acquisition system consisted of a camera (Sony XC-003P), a lighting system composed of eight fluorescent tubes (Philips daylight, 25 w) and polarised filters in order to avoid bright spots in the scene. The acquisition of the NIR images was performed using a Hamamatsu BeamFinder III C5332-01 camera, sensitive from 400 nm to 1800 nm. The lighting system was made up of two incandescent lamps (Philips R125-IR, 250 w). To prevent interference of visible information, a 700 nm cut-band filter was coupled to the camera lens. The fluorescence images were acquired using the same camera that was employed to acquire the colour images. In this case, the fruits were illuminated using black light fluorescent tubes (18 W each) that emit radiation with a wavelength between 350 nm and 400 nm, with a peak at 370 nm. Unlike the work presented by Blasco *et al.* (2007a), the fluorescence images were acquired using only the G video signal. This represents an important advantage with respect to the previous system

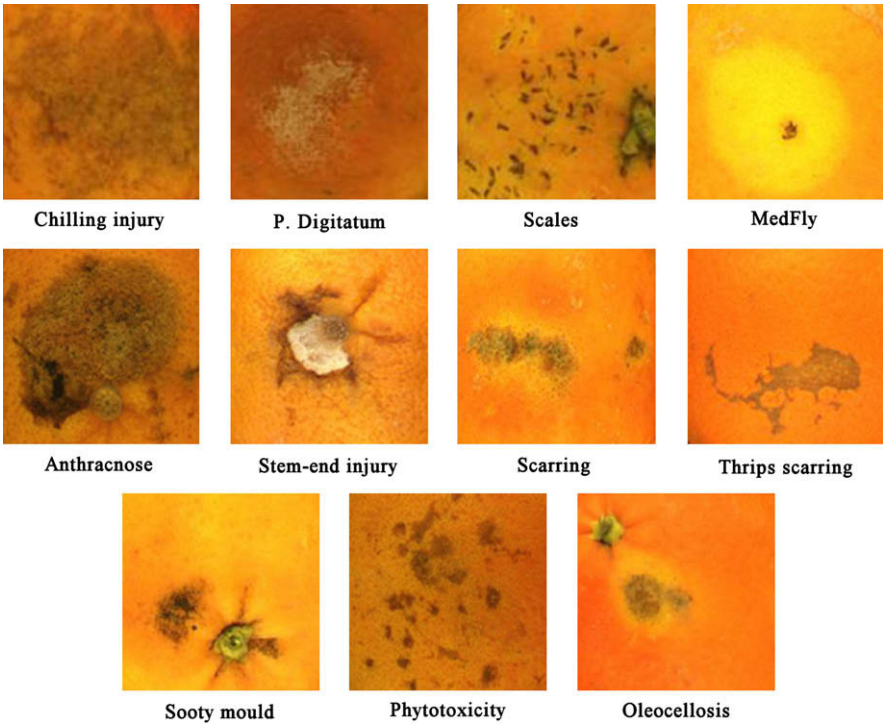

Fig. 1 – Representative details of the actual size, shape and colour of the defects that were studied.

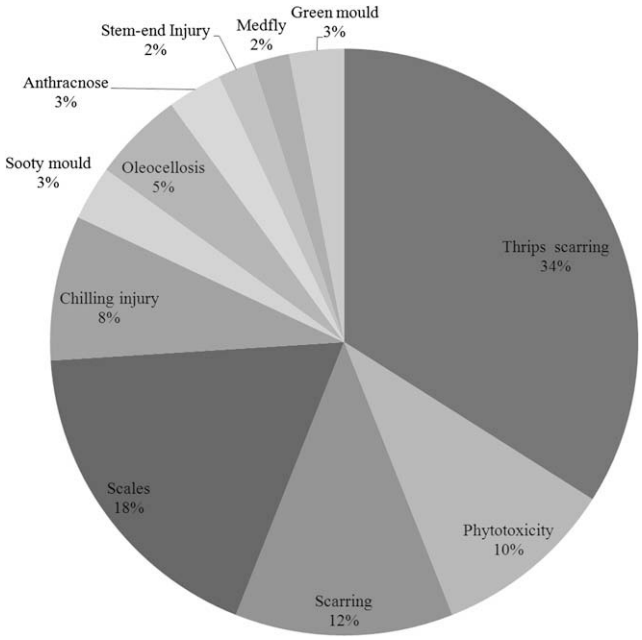

Fig. 2 – Frequency distribution of the defects that were studied.

since the use of external filters blocks part of the light, thus resulting in a loss of contrast in the image. The computer used to process the images was based on an Intel Pentium Core 2 duo processor with 2048 Mb of RAM (Random Access Memory) mounted with a frame grabber to digitise the images (Matrox Meteor II). In all cases, images containing one entire fruit (with a size of 768×576 pixels, a spatial resolution of about 0.17 mm pixel^{-1} and a colour depth of 2^8 bits) were acquired off-line by manually presenting the side of the fruit that contained the defects to the camera. The images were acquired using the standard CCIR (Comité Consultatif International des Radiocommunications) video signal without employing a shutter, the acquisition time being 40 ms.

3.3. *Problems related with the geometrical shape of the fruits*

Spherical fruits have the particular problem that luminosity decreases towards their borders. Various attempts have been made to solve this problem by applying spherical models with a constant curvature and variable radii Wen and Tao (1999). Another solution that has traditionally been employed to lessen this problem is to erode the outline of the fruit (Blasco *et al.*, 2003; Kleynen *et al.*, 2005), but this involves a loss of quality in the inspection because sometimes an important part of the fruit surface is not analysed. Other attempts use the image of a reference fruit to calculate and correct the darkening near the edges (Li *et al.*, 2002). Another approach consists of assigning the same physical region to different classes, for example, by assigning different classes for the healthy skin depending on the area of the fruit that is being segmented. This solution offers a number of drawbacks in multiclass problems because most classifiers reduce their success rate as the number of classes increases (Duda and Hart, 1973). The solution of correcting the reflectance by estimating the size and curvature of the fruit was studied by Gómez-Sanchis *et al.* (2008b). In this study, the problem was not present in the UVFL images because all the fruit appears completely dark except for the fluorescent damaged area. In the case of the visible RGB images, the lighting system minimised the problem by being set up in such a way as to surround the fruit, although the boundaries still appeared darker than the top of the fruit. The greatest problems occurred in NIR images because the lamps used were placed at an angle of 45° with respect to the plane of the camera and produced shadows near the boundaries. However, NIR reflectance of fruit is very highly contrasted with the reflection from the background. Furthermore, there is also a greater contrast between the reflection of the sound fruit and the reflection of the defects detected in these images, thus doing away with the need to make particular corrections.

For on-line operation, fruit should rotate while being transported under the camera to maximise the surface inspected, as in the work presented by Bennedsen *et al.* (2005). However, in this case, the fruits were placed manually below the camera, since the aim was to develop an algorithm capable of identifying the defects as a preliminary step to developing a real-time automatic system.

3.4. *Segmentation of the images*

The colour image is segmented using the method described in Blasco *et al.* (2007b), which is aimed at detecting the defects in the fruits, separating them from the healthy skin. It consists of a region-growing algorithm that selects a set of 'seeds' in the image by following a specific criterion. In this case the seeds were chosen in the areas of the image with the most uniform colour. The neighbouring pixels that meet certain conditions are added to these regions through an iterative process that ends when all the pixels in the image belong to one region. The next step is to merge regions. We used an approach based on similarity of colour, as the HSL (Hue, Saturation, Lightness) colour space utilised is uniform and appropriate for the estimation of colour differences. Once the image is segmented, we obtain a collection of unlabelled regions, of which the largest is assumed to correspond to healthy skin, while the remaining smaller regions are considered to be defects.

The NIR and UVFL images presented similar features. In both, the fruits appeared clearly separated from the background with relatively little noise. In preliminary tests it was observed that only anthracnose and sooty mould were shown in NIR images and only decay appeared in the fluorescence images, these defects being well contrasted against the background and the surrounding sound skin. Other defects could appear as noise in the original image, looking like small blurred shadows that did not affect segmentation.

The algorithm developed for the segmentation of the NIR and fluorescence images is based on the analysis of the histogram. In both images, the background is homogeneously dark. In the UVFL images, the sound skin is practically as dark as the background. If there is no defect present in the fruit, the images appear totally black. For these images, the histogram shows one peak near zero, corresponding to the background and sound peel, and another peak for the defects. To obtain

a dynamic threshold for binarising the image (by setting the pixels of the background and sound peel to zero and the pixels of the defects to a value of 255), the algorithm coded the profile of the histogram using a run-length code and then sought a relative minimum between the peaks of the sound skin and the defects. Figure 3 shows a typical histogram of an image of a fruit with a small decay blemish, acquired using the G channel of the camera employed in the fluorescence system. The two peaks can be clearly seen.

The case of NIR images is more complex, since the grey level value of the background is similar to the grey level value of some defects, thereby making it difficult to separate them using a threshold. In this case we need a two-step segmentation process. The first step separates the fruit and the background. The pixels in both regions are quite highly contrasted, which makes it possible to use the above-mentioned technique of searching for a dynamic threshold between the two peaks of the histogram. The result is a region corresponding to the fruit that is segmented with blobs inside it, which correspond to the defects (if any). A second operation is performed to search for blobs inside the fruit. This two-step technique has previously been used in similar cases, such as those described by Leemans and Destain (2004), who also analyse blobs inside the fruit region or the solution by Unay and Gosselin (2006), who simply fill the blobs using morphological operations. Sophisticated segmentation algorithms could probably be applied to solve this problem, such as the three methods described by Bennedsen *et al.* (2005), but in our case the defects and the sound peel were well contrasted and the solution reported here yielded good results.

3.5. *Morphological analysis of defects*

Once the image has been segmented, the shape analysis sequence starts with the extraction of the perimeter (*P*) of the objects of interest (the closed contour), which is formed by the pixels belonging to the object that have some neighbour that is part of the background. Then, the centroid is calculated as the average *x* and *y* coordinates of the pixels in the perimeter. The area (*A*) is calculated as the number of pixels inside the perimeter:

$$A = \sum_{x} \sum_{y} I(x,y) \tag{1}$$

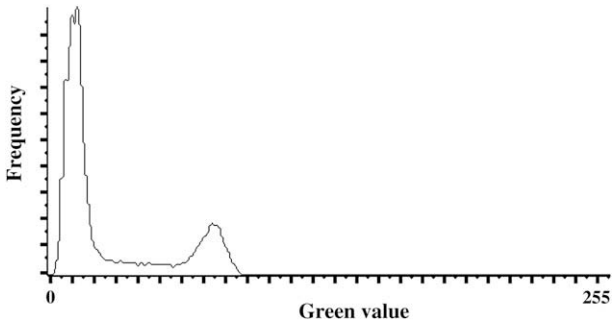

Fig. 3 – Histogram of a fluorescence image of a decayed orange. The highest peak corresponds to the pixels of the sound skin and the smaller one to the pixels belonging to the damage.

where $I(x,y) = 1$ if the pixel in position (x,y) belongs to the region and $I(x,y) = 0$ otherwise.

The moments of inertia are calculated following the equations described by Tanenbaum (2004). The principal axis of inertia is used to estimate the length and width of the objects, which are in turn used to estimate the elongation (E), taken as the ratio between the length (L) and width (W) of the object.

$$E = W \cdot L^{-1} \tag{2}$$

Finally, the contour is coded using the radius signature, which is a one-dimensional array containing the Euclidean distance between the centroid of the object and each point on the contour $p(i)$ $i = [0,P]$. Fourier analysis allows any wave form to be represented using a set of harmonically related components with a suitable amplitude and phase (González and Woods, 2002). The result of applying the FFT algorithm to a contour is a set of values corresponding to the fundamental frequency and to the harmonics of the shape. In this work FFT of this signature is calculated because it provides information about the profile which can be used as an estimation of the shape of the defects (Tao *et al.*, 1995). Following this research, the first 10 harmonics were used to describe the shape of the defects. Figure 4 shows an example this signature. The shape of a typical defect caused by thrips is shown on the left. Starting at the top point, the boundary is performed clockwise. The graph on the right shows the Euclidean distance between each point on the perimeter and the central point of the defect.

3.6. *Classification of defects*

The probability of a region of interest in the segmented image being identified as a particular defect is estimated through Bayes theorem. This allows the *a posteriori* probability $P(w_i|x)$ of a pattern x formed by a set of j features $(x_1 \ldots x_j)$ belonging to any of the N classes w_i to be calculated from the *a priori* $P(w_i)$ and the conditional $P(x|w_i)$ probabilities. In our particular case, the features are composed of the colour coordinates and the morphological features extracted for each region, which are the independent variables in the statistical analysis that is performed in order to classify the regions as particular defects. A standard non-linear Bayesian discriminant analysis was used to determine the classification functions. Thus, a classification function was obtained for each class which maximises its value when a sample is assigned to its corresponding class. Assuming the cost of a classification error to be equal for each class, the maximisation function is defined as (3):

$$P(w_i|x) = \frac{p(x|w_i)P(w_i)}{\sum_{j=1}^{m} p(x|w_j)P(w_j)}; i = 1, \ldots m \tag{3}$$

where m is the number of classes (the 11 defects), x is the n-dimensional observed vector of a defect, w_i $(i = 1 \ldots m)$ is one of the m different classes and $P(w_i)$ is the *a priori* probability of a particular combination of features pertaining to a specific class (without knowing its observed vector). In our implementation, this probability is the same for each class.

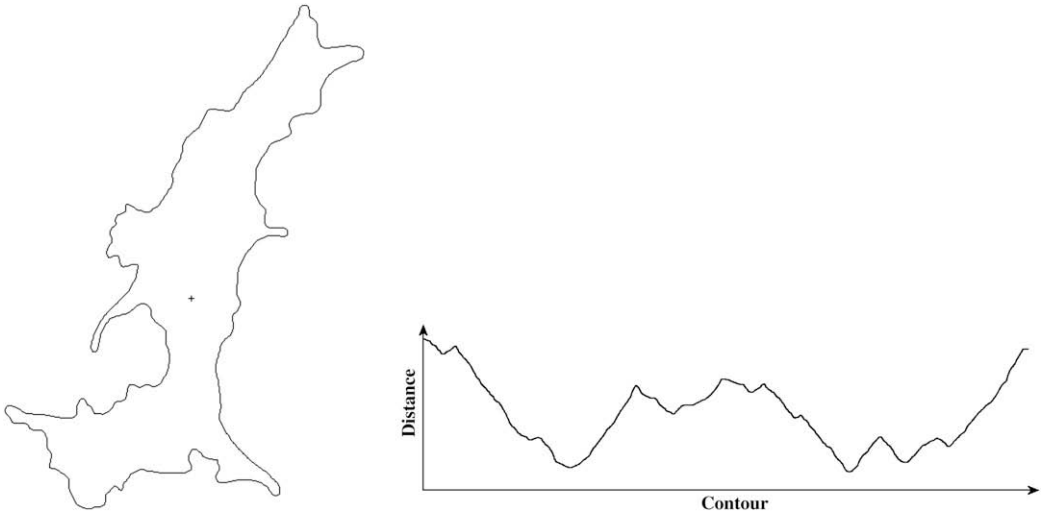

Fig. 4 – Image of the boundary of a defect caused by thrips (left); graph of the radius signature (right).

If we consider $p(x|w_i)$ to be the conditional density function of an observed vector x pertaining to the class w_i, then $P(w_i|x)$ is the probability of the observed vector of a feature pertaining to the class w_i. A region, whose observed vector is x, pertains to the class w_i if:

$$\forall j \neq i, P(w_i|x) > P(w_j|x), \quad i, j \in [1, m] \tag{4}$$

Substituting in (4):

$$\forall j \neq i, p(x|w_i)P(w_i) > p(x|w_j)P(w_j) \tag{5}$$

Assuming normal distribution of density functions, $p(x|w_i)$ is equal to:

$$p(x|w_i) = \frac{e^{-1/2(x-\mu_i)^T C_i^{-1}(x-\mu_i)}}{(2\pi)^{m/2}\left|C_i\right|^{-1/2}} \tag{6}$$

where μ_i, C_i and C_i^{-1} are the mean, the covariate matrix and the covariate inverse matrix of the class i respectively, estimated using the training set of images. The m value will coincide with the dimension of the vector x. It can be seen that the Mahalanobis distance appears in the numerator.

Only the training set of images was used to build the statistical model, after first being segmented as described. Bearing in mind the conclusions presented by Blasco *et al.* (2007a), the colour information obtained from the HSL coordinates was collected from pixels representing each type of blemish, which were manually selected and labelled using the computer mouse. The colour coordinates and a label indicating the type of defect were stored for each pixel. This task was performed using only the training set of images, which contained an extensive variety of all types of defects. The training set of data was complemented with the area, elongation and the first 10 Fourier coefficients of each defect extracted from the contour signature. These features were used as independent variables to perform a Bayesian discriminant analysis with the aim of obtaining the classification functions (Duda and Hart, 1973). The label with the type of defect was used as the grouping variable. For each segmented region, the probability of the observed vector (that consisted of the described features) being a particular defect was estimated through the classification functions, and then assigned to the defect with the highest value.

3.7. *Algorithm for sorting the fruit*

The proposed algorithm is intended for classifying defects, the result being the type of the defect that affects a particular fruit. Both visible and non-visible information are combined in this algorithm to obtain a citrus fruit-sorting system. The citrus classification algorithm (Fig. 5) proposed here allows prior detection of serious defects that can prevent the fruits from being commercialised. If no objects of interest other than sound skin are found during the segmentation process, the fruit is considered to be sound and the process finishes. Otherwise, the algorithm is applied to determine the type of damage.

The first images to be analysed are those that allow the detection of decay, which are the images acquired under UVFL. It is important to detect and remove these fruits in order to prevent the defect from spreading to other sound fruits. Segmentation is performed by searching for a dynamic threshold between the defect and the rest of the image following the technique described above. If two peaks are found in the histogram, then this means that a defect is present. Since only decay can be detected in these images, the fruit is automatically sorted as decayed and the algorithm finishes. Otherwise, the algorithm continues to search for other types of defects.

The next images to be analysed are those acquired from NIR to detect anthracnose and sooty mould. If any defect is found, it is assumed to be one of these two types of defects. However, in these images it is not possible to distinguish between these two defects, so the algorithm then continues but only to discriminate between them by using the colour information. If no defects are detected in the NIR and UVFL images, then the colour and the morphological features are used to determine which type of defect is affecting the fruit using the Bayesian classifier. If no defects are found in the RGB images, the fruit is classified as sound fruit; otherwise the classifier will return a type of defect for any of the regions

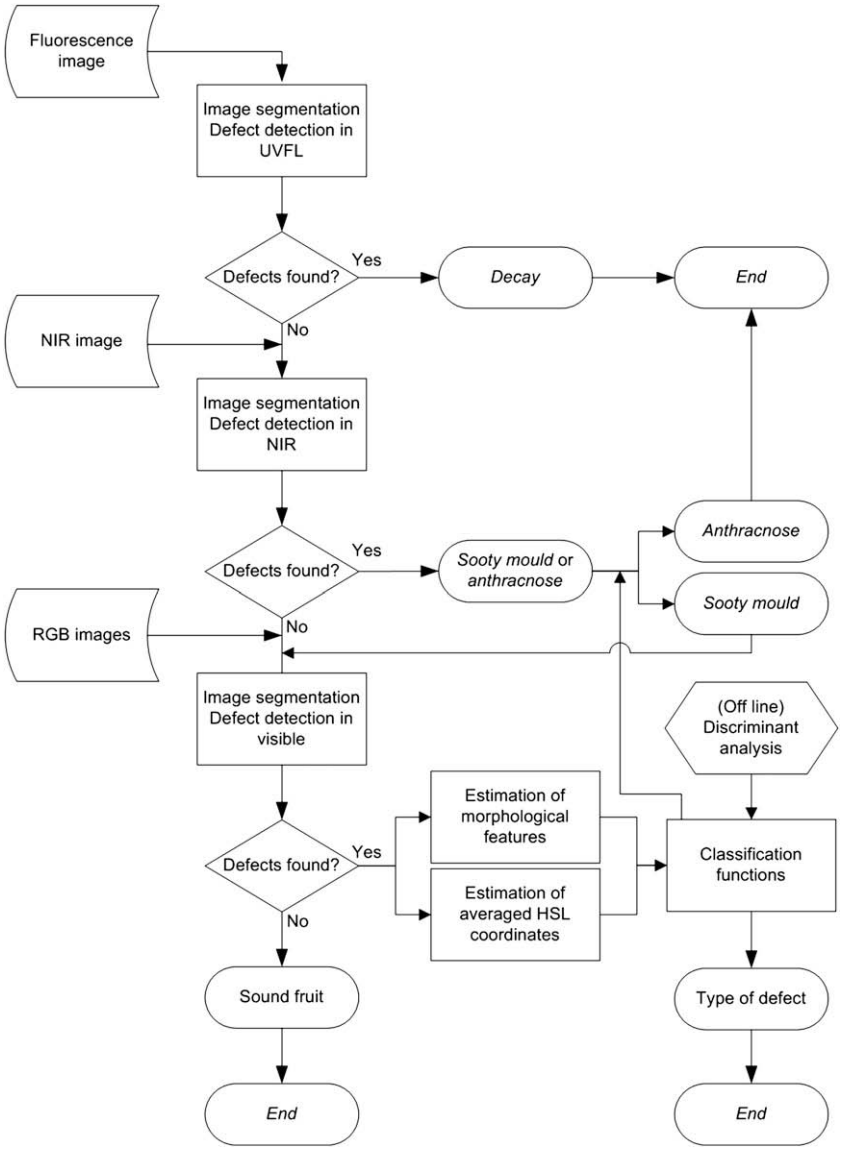

Fig. 5 – Flowchart of the algorithm for the identification of defects in citrus fruits.

segmented as defects and the fruit will be classified in terms of the largest defect. If one of these defects is considered to be severe, such as green mould, medfly, anthracnose, decay or stem-end injury, the fruit is considered as non-marketable.

In order to measure the speed of image processing, an oscilloscope was connected to the parallel port of the vision computer. At the beginning of the image analysis, the machine vision computer triggered the oscilloscope time counter. At the end of the image processing, a new signal stopped the clock, thus allowing us to measure the time that had elapsed.

4. Results and discussion

4.1. *Recognition of defects*

Using only colour information, the system can process the images quickly, since the detection can be performed together with the segmentation process without further time-consuming operations. However, as stated by Blasco *et al.* (2007a) there are defects with very similar colours that can be confused. Typical cases were found to be defects caused by scales, which are most commonly confused with thrips (29% of misclassification), or scarring (5% of misclassification). The data shows that only 65% of defects could be properly identified using only colour information. On introducing the morphological parameters presented in this article, the correct classification rate reached 82% since there is a great difference in the size and shape of these defects.

By introducing NIR and UVFL images in the analysis, success rate increases to reach 86%. However, beyond the numerical results, the greatest increment was achieved in the identification of anthracnose and green mould (95% and 97%, respectively), which are dangerous defects that spread the disease to sound fruits and their identification must be maximised. Table 1 shows the confusion matrix for the classification of the 11 types

Table 1 – Confusion matrix for the classification obtained by the system

Detected	Actual											
	Thrips	Phyto-toxicity	Scarring	Scales	Chilling injury	Sooty mould	Oleo-cellosis	Anthra-cnose	Stem-end injury	Medfly	Green mould	Reliability
Thrips	86	9	15	7	0	0	2	0	0	0	0	72
Phytotoxicity	0	82	1	2	0	0	4	0	0	5	0	87
Scarring	10	0	81	5	0	0	2	0	0	0	0	83
Scales	0	0	0	84	0	0	0	0	0	0	0	100
Chilling injury	4	7	3	0	100	0	6	0	0	0	0	83
Sooty mould	0	0	0	0	0	91	0	5	0	0	0	95
Oleocellosis	0	0	0	0	0	0	66	0	4	17	1	75
Anthracnose	0	0	0	0	0	9	0	95	0	5	0	87
Stem-end injury	0	0	0	0	0	0	0	0	96	0	0	100
Medfly	0	2	0	2	0	0	9	0	0	73	2	83
Green mould	0	0	0	0	0	0	11	0	0	0	97	90

of defects, the average rate of successful identification being 86%. Several assessment measures can be obtained from these matrices (Congalton and Green, 1999). The proposed algorithm not only performs well in terms of overall accuracy but is also robust as regards the Fleiss' kappa statistic (Fleiss, 1971; Sim and Wright, 2005), which takes a value of 0.74 with a variation of the estimated kappa statistics of 1.33×10^{-4} and a confidence interval of 0.045. These numerical and statistical results can be explained by inspecting the confusion matrices in greater detail. More particularly, the greatest confusion is obtained in defects with similar sizes such as thrips or scarring and medfly or oleocellosis.

Nowadays no commercial systems for automatic fruit inspection are capable of identifying the different types of defects present in the skin of the fruits, being only capable of detecting their presence but not discriminating among them. After solving the problem of the natural colour and the great variability of shapes, colours and sizes of the defects under study and bearing in mind that the number of classes to be classified is relatively large, a correct classification rate of 86% can be considered to be a good result. The use of the green channel of a colour camera to obtain the fluorescence images instead of using the three channels and an external filter coupled to the camera optics reduces the complexity of the equipment and allows images with a higher contrast to be obtained, thus increasing the detection of decay, which is probably the most important defect from the commercial point of view.

A major problem concerning the implementation of this algorithm on-line is the large amount of processing time it requires. Although the images should be acquired by different cameras, these tasks can be overlapped in time in such a way that while one image is being acquired, another can be processed. The algorithm developed allows this methodology if the order is: UVFL, NIR and RGB. But processing all the images is still time consuming and expensive. NIR and RGB images can be acquired simultaneously, as demonstrated in Aleixos *et al.* (2002), by implementing a camera capable of acquiring both images at the same time. In the case of UVFL images, the importance of detecting decay is very high because it can spread to other fruits during their storage or transport. Packing houses have special locations where the fruits are inspected manually under UV radiation to detect this particular defect. These results could be the basis for developing an automatic machine designed for this purpose.

A possible on-line system could be formed by two consecutive inspection chambers, one for colour and NIR and the other for fluorescence. Fruit would be transported by double-tapered rollers that carry the fruits under the camera while making them rotate, thereby presenting most of the surface to the camera while the fruit crosses the inspection area. This transport system is already common in commercial machines for colour or diameter measurement. The main obstacle today is the amount of time needed to perform the processing of the growing region. When this work began, this operation required 45 s per image (using a Pentium III 600 MHz processor and 128 Mb of RAM). Nowadays, this time has been reduced to less than 1 s by optimising the algorithms and using more advanced computing technology (Pentium Core 2 duo 3.00 GHz, 2048 Mb of RAM). Although this is still too much time to be implemented in a commercial system (which requires a processing time below to 100 ms per image) we are closer to achieving this goal.

4.2. *Detection of serious diseases*

One of the aims of this work is to try to evaluate the ability of this system to separate fruits with serious diseases from those with slight external defects. Serious diseases that can be disseminated during the packing, storage and marketing of the fruit are related with decay or damage that can facilitate the development of further rotting. Of the defects under study here, these are: anthracnose, stem-end injury, medfly egg deposition and green mould. Table 2 shows the discrimination achieved between these two types of defects. A total of 6% of

Table 2 – Capability of the system to distinguish between serious diseases and slight defects

Detected	Actual	
	Slight defects	Serious defects
Slight defects	98%	6%
Serious defects	2%	94%

serious diseases are confused with slight defects, the commonest case being the false detection of the defect caused by medfly as oleocellosis. On the other hand, 98% of slight defects were correctly identified.

5. Conclusions

The system proposed here can successfully discriminate between 11 defects in 86% of cases. Using only visible information, the results are also acceptable (82%) but the confusion between serious and slight defects increases since green mould can be detected using UVFL in 97% of cases and anthracnose can be detected using NIR in 95% of cases.

A fruit-sorting algorithm that combines visible and non-visible information together with morphological features has been proposed. The contribution of NIR and UVFL played an important role in the detection of serious diseases such as anthracnose and decay as discussed, both of which are considered to be serious types of damage. Serious defects were successfully discriminated in 94% of cases, most errors being due to confusion between those caused by medfly and oleocellosis, since they can present similar shapes and colours as can be seen in Fig. 1.

Reducing the processing time is still a challenge, since it is too high to allow this algorithm to be implemented in a real-time system. However, further advances in technology can help this to be achieved.

Acknowledgments

This work was partially funded by the Spanish Ministry of Education (MEC) and by European FEDER funds, through projects DPI-2003-09173-C02-02 and DPI-2007-66596-C02-02.

REFERENCES

Alchanatis V; Peleg K; Ziv M (1999). Classification of tissue culture segments by colour machine vision. Journal of Agricultural Engineering Research, **55**, 299–311.

Aleixos N; Blasco J; Navarrón F; Moltó E (2002). Multispectral inspection of citrus in real-time using machine vision and digital signal processors. Computers and Electronics in Agriculture, **33**(2), 121–137.

Al-Mallahi A; Kataoka T; Okamoto H (2008). Discrimination between potato tubers and clods by detecting the significant wavebands. Biosystems Engineering, **100**(3), 329–337.

Ariana D; Guyer D E; Shrestha S (2006). Integrating multispectral reflectance and fluorescence imaging for defect detection on apples. Computers and Electronics in Agriculture, **50**, 148–161.

Batchelor B G; Whelan P F (1995). Real-time colour recognition in symbolic programming for machine vision systems. Machine Vision and Applications, **8**(6), 385–398.

Bennedsen B S; Peterson D L; Tabb A (2005). Identifying defects in images of rotating apples. Computers and Electronics in Agriculture, **48**(2), 92–102.

Bennedsen B S; Peterson D L (2005). Performance of a system for apple surface defect identification in near-infrared images. Biosystems Engineering, **90**(4), 419–431.

Blasco J; Aleixos N; Roger J M; Rabatel G; Moltó E (2002). Robotic weed control using machine vision. Biosystems Engineering, **83**(2), 149–157.

Blasco J; Aleixos N; Moltó E (2003). Machine vision system for automatic quality grading of fruit. Biosystems Engineering, **85**(4), 415–423.

Blasco J; Aleixos N; Gómez J; Moltó E (2007a). Citrus sorting by identification of the most common defects using multispectral computer vision. Journal of Food Engineering, **83**(3), 384–393.

Blasco J; Aleixos N; Moltó E (2007b). Computer vision detection of peel defects in citrus by means of a region oriented segmentation algorithm. Journal of Food Engineering, **81**(3), 535–543.

Congalton R G; Green K (1999). Assessing the Accuracy of Remotely Sensed Data: Principles and Practice. Mapping Sciences Series. CRC Press Inc, New York (USA).

Duda R O; Hart P E (1973). Pattern Classification and Scene Analysis. John Willey & Sons, New York (USA).

Fleiss J L (1971). Measuring nominal scale agreement among many raters. Psychological Bulletin, **76**(5), 378–382.

Gómez-Sanchis J; Gómez-Chova L; Aleixos N; Camps-Valls G; Montesinos-Herrero C; Moltó E; Blasco J (2008a). Hyperspectral system for early detection of rottenness caused by Penicillium digitatum in mandarins. Journal of Food Engineering, **89**(1), 80–86.

Gómez-Sanchis J; Moltó E; Camps-Valls G; Gómez-Chova L; Aleixos N; Blasco J (2008b). Automatic correction of the effects of the light source on spherical objects. An application to the analysis of hyperspectral images of citrus fruits. Journal of Food Engineering, **85**(2), 191–200.

Gonzalez R C; Woods R E (2002). Digital Image Processing (second ed.). Prentice Hall, UpperSaddle River, NJ (USA).

Kleynen O; Leemans V; Destain M F (2005). Development of a multi-spectral vision system for the detection of defects on apples. Journal of Food Engineering, **69**, 41–49.

Leemans V; Destain M F (2004). A real-time grading method of apples based on features extracted from defects. Journal of Food Engineering, **61**, 83–89.

Li Q; Wang M; Gu W (2002). Computer vision based system for apple surface defect detection. Computers and Electronics in Agriculture, **36**, 215–223.

Mehl P M; Chao K; Kim M; Chen Y R (2000). Detection of defects on selected apple cultivars using hyperspectral and multispectral image analysis. Applied Engineering in Agriculture, **18**(2), 219–226.

Ponsa D; Benavente R; Lumbreras F; Martínez J; Roca X (2003). Quality control of safety belts by machine vision inspection for real-time production. Optical Engineering, **42**(4), 1114–1120.

Sim J; Wright C C (2005). The kappa statistic in reliability studies: use, interpretation, and sample size requirements. Physical Therapy, **85**(3), 206–282.

Tao Y; Morrow C T; Heinemann P H; Sommer H J (1995). Fourier-based separation technique for shape grading of potatoes using machine vision. Transactions of the ASAE, **38**(3), 949–957.

Tenenbaum R A (2004). Fundamentals of Applied Dynamics. Springer, New York, (USA).

Unay D; Gosselin B (2006). Automatic defect segmentation of 'Jonagold' apples on multi-spectral images: a comparative study. Postharvest Biology and Technology, **42**, 271–279.

Wen Z; Tao Y (1999). Building rule-based machine vision system for defect inspection on apple sorting and packing lines. Expert Systems with Applications, **16**, 307–313.

Zheng C; Sun D W; Zheng L (2006). Recent developments and applications of image features for food quality evaluation and inspection e a review. Trends in Food Science & Technology, **17**, 642–655.